

# Computing pseudo-shear-wave data using PP and PS-wave traveltimes in the rayparameter domain

Raul Cova and Kris Innanen

## ABSTRACT

The kinematics of converted-waves is one of the features that complicates the processing of multicomponent data. The asymmetry of the converted-wave raypath prevents us from using an important part of the methods developed for P-wave processing. To accommodate the issue of asymmetric raypath Grechka and Tsvankin (2002) and Grechka and Dewangan (2003) proposed what they named the PP+PS=SS method. Their goal was to generate pseudo-shear-wave data by convolution and correlation of PP and PS-wave data. By taking advantage of the shared raypath between PS and PP data in the space domain they were able to retrieve the kinematics of pure shear-wave data. Here, we propose moving the data to the plane-wave domain, where the shared features of PS and PP are more evident. Although the P and S-leg of converted-wave events may follow different raypath angles, they share the same rayparameter following Snell's law. Recently, Tao and Sen (2013) developed a mathematical framework for doing interferometry in the plane-wave domain. They showed how the cross correlation-type reciprocity equation holds for data in the rayparameter domain. Hence, data with shared rayparameters can be cross correlated to get redatumed data. In this work I will be using seismic interferometry in the plane-wave domain to extend the PP+PS=SS method to this framework. Access to the rayparameter values will be achieved by the  $\tau$ - $p$  transform and cross correlation and convolution of PS and PP data will be performed to reconstruct the kinematics of pure S-wave data.

## Interferometry in the plane-wave domain

Plane wave interferometry uses the  $\tau$ - $p$  transform or "slant-stack" transform to compute the ray parameter values ( $p$ ) present in the data (Claerbout, 1975; Stoffa, 1989). In the space-time ( $x$ - $t$ ) domain the  $\tau$ - $p$  transform stacks data along straight lines given by the equation  $t = \tau + px$ , where  $\tau$  is the intercept time and  $x$  is the offset. In the frequency domain the  $\tau$ - $p$  transformation is achieved by phase-shifts followed by summation in the space coordinate. Equation 1 shows the expression for transforming shot gather data into the  $\tau$ - $p$  domain.

$$\hat{D}(x_s|p_r, \omega) = \int D(x_s|x_r, \omega) e^{i\omega p_r x_r} dx_r, \quad (1)$$

where  $D(x_s|x_r, \omega)$  is the recorded data in the frequency domain,  $x_s$  is the source position,  $x_r$  is the receiver position,  $p_r$  is the receiver ray parameter, and  $\hat{D}(x_s|p_r, \omega)$  is the transformed plane-wave gather from the original shot gather.

The inverse  $\tau$ - $p$  transform is given by,

$$D(x_s|x_r, \omega) = \omega^2 \int \hat{D}(x_s|p_r, \omega) e^{-i\omega p_r x_r} dp_r. \quad (2)$$

For a receiver gather the same equations hold but integration is performed over the shot position coordinate ( $x_s$ ) and shot-ray-parameter values ( $p_s$ ).

Seismic interferometry as introduced by Wapenaar (2004) and Schuster (2009) is based in the cross correlation of frequency domain data and integration over the location coordinates in order to retrieve or redatum data at different spatial locations. Equation 3 shows the so called reciprocity equation of the correlation type after considering far field conditions and ignoring amplitude effects.

$$\text{Im} [D(x_B|x_A, \omega)] \approx \int D(x|x_A, \omega)D(x|x_B, \omega)^* dx. \quad (3)$$

From equation 2 the complex conjugate of the data at the  $x_B$  location can be written as,

$$D(x|x_B, \omega)^* = \omega^2 \int \hat{D}(x_B|p, \omega)^* e^{i\omega px} dp. \quad (4)$$

Substituting equation 4 into equation 3 results in,

$$\text{Im} [D(x_B|x_A, \omega)] \approx \omega^2 \int \int D(x|x_A, \omega) \hat{D}(x_B|p, \omega)^* e^{i\omega px} dp dx. \quad (5)$$

Rearranging equation 5 we get,

$$\text{Im} [D(x_B|x_A, \omega)] \approx \omega^2 \int \hat{D}(x_B|p, \omega)^* dp \int D(x|x_A, \omega) e^{i\omega px} dx. \quad (6)$$

Notice that the rightmost integral is the forward  $\tau$ - $p$  transform (equation 1) of the data at location A. Therefore, equation 6 gives,

$$\text{Im} [D(x_B|x_A, \omega)] \approx \omega^2 \int \hat{D}(x_B|p, \omega)^* \hat{D}(x_A|p, \omega) dp. \quad (7)$$

Equation 7 suggests that, similar to cross correlation and sum over trace locations to cancel out shared raypaths, in the  $\tau$ - $p$  domain this can be achieved by cross correlation and summation over rayparameter values. Figure 1 depicts this idea. Since the direct ray from the source location S\* to the receiver location A, has the same ray parameter as the event S\*AOB, the traveltimes along the shared raypath are cancelled out by the cross correlation. The output is a trace whose source appears to be at location A and whose receiver is located at B.

### Convolution-type interferometry in the plane-wave domain

A normalized version of the convolution-type reciprocity equation (Schuster, 2009; Wapenaar et al., 2011) can be written as,

$$D(x_B|x_A, \omega) \approx \int D(x|x_A, \omega)D(x|x_B, \omega)dx. \quad (8)$$

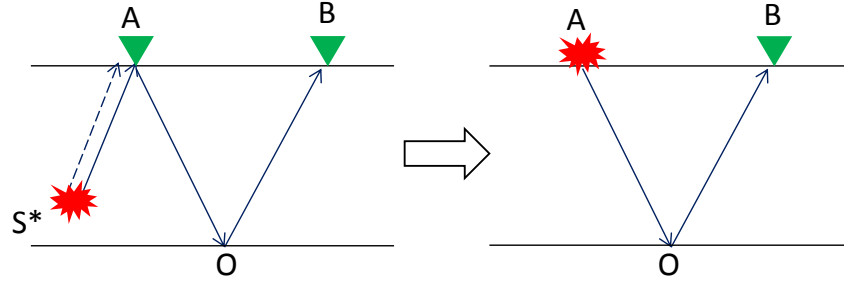


FIG. 1. Sketch showing how the cross correlation of the direct arrival from the stationary source position  $S^*$  with the raypath  $S^*AOB$  cancels out the shared raypath  $S^*A$  retrieving the traveltimes as if the source had been in at the location A. In the  $\tau$ - $p$  domain this cancellation is possible since the raypaths share the same rayparameter.

Note that instead of multiplication with a complex conjugate, in the convolution-type interferometry we get a simple multiplication. As a result the phases of the functions inside the integral are summed producing a new function with longer traveltimes.

Replacing the functions inside equation 8 by their inverse  $\tau$ - $p$  transforms we get,

$$D(x_B|x_A, \omega) \approx \int \left[ \omega^2 \int \hat{D}(x_A|p, \omega) e^{-i\omega p x} dp \right] \left[ \omega^2 \int \hat{D}(x_B|p', \omega) e^{-i\omega p' x} dp' \right] dx, \quad (9)$$

Changing integration orders and adding the phases,

$$D(x_B|x_A, \omega) \approx \int \int \omega^4 \hat{D}(x_A|p, \omega) \hat{D}(x_B|p', \omega) dp dp' \int e^{-ix\omega(p'+p)} dx, \quad (10)$$

The rightmost integral can be identified as a scaled delta function. Hence, equation 10 becomes,

$$D(x_B|x_A, \omega) \approx \int \int \omega^4 \hat{D}(x_A|p, \omega) \hat{D}(x_B|p', \omega) \left[ \frac{2\pi}{\omega} \delta(p' + p) \right] dp dp', \quad (11)$$

Using the sifting property of the delta function after integrating over  $p'$ ,

$$D(x_B|x_A, \omega) \approx 2\pi\omega^3 \int \hat{D}(x_A|p, \omega) \hat{D}(x_B| -p, \omega) dp. \quad (12)$$

Figure 2 shows how the addition of traveltimes along two raypaths with the same ray-parameter value but pointing in opposite directions may return the two-way traveltimes of a reflection-like event. This depicts the result given in equation 12

### The PP+PS=SS method

The PP+PS=SS method was introduced by Grechka and Tsvankin (2002) and Grechka and Dewangan (2003) as a tool for computing pseudo-shear-wave data as an alternative to

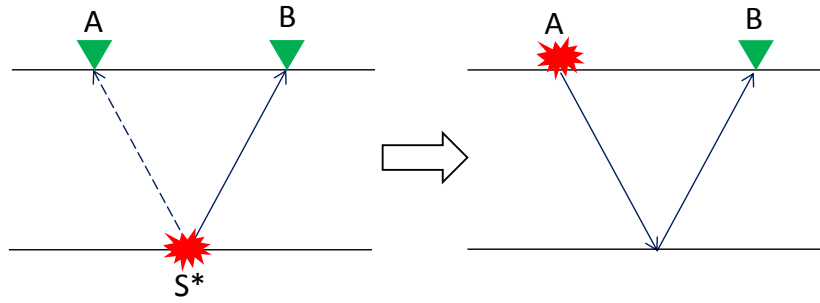


FIG. 2. Sketch showing how the addition of the traveltimes from the source location  $S^*$  to receivers A and B, leads to the two way traveltimes as if the source had been in location A. Since the convolution happens between rays with the same rayparameter but in opposite directions the resulting raypath is symmetric as in a pure-P or pure-S-wave reflections.

processing converted-waves. The method they proposed is clearly related to the cross correlation methods nowadays known as seismic interferometry. Figure 3 shows the rationale behind the PP+PS method. There, the raypaths AOD and BOC represent PS events and the raypath AOB is a PP reflection. Based on this construction the shear-wave traveltime  $t_{SS}(C, D)$  can be computed as:

$$t_{SS}(C, D) = t_{PS}(A, D) - t_{PP}(A, B) + t_{PS}(B, C) \quad (13)$$

The traveltime in equation 13 can also be retrieved by cross correlation (traveltime subtraction) and convolution (traveltime addition) as expressed in equation 14.

$$d_{\Psi S}(x_C|x_D, t) = \int \int [d_{PS}(x_A|x_D, t) * d_{PP}(x_A|x_B, t)^* * d_{PS}(x_B|x_C, t)] dx_A dx_B \quad (14)$$

where  $d_{PS}(x_A|x_D, t)$  and  $d_{PS}(x_B|x_C, t)$  are the PS data recorded at locations  $(x_A|x_D)$  and  $(x_B|x_C)$  respectively,  $d_{PP}(x_A|x_B, t)^*$  denotes the complex conjugate of the PP data with  $(x_A|x_B)$  coordinates,  $d_{\Psi S}(x_C|x_D, t)$  is the pseudo-shear-wave data recorded between locations  $(x_C|x_D)$  and the  $*$  symbol indicates time convolution. Notice, that time convolution with the complex conjugate of the PP data is equivalent to time cross correlation.

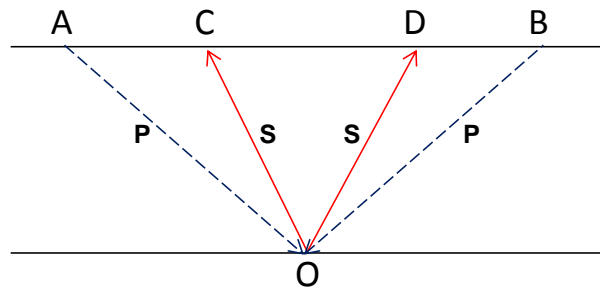


FIG. 3. Geometry of the reconstruction of SS traveltimes by using the PP+PS=SS method. AOD and BOC represent converted-wave events and AOB depicts a PP reflection.

As we can see the PP+PS=SS method is posed in the x-t domain. Integration over the  $x_A$  and  $x_B$  coordinates assures finding the stationary locations where the raypath of the PP data overlaps the P-legs of the PS data. During integration, the authors propose using only the data with half-offsets shorter than the critical PS offset.

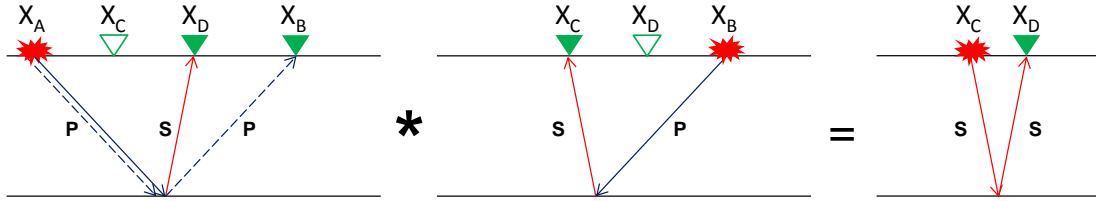


FIG. 4. Representation of the correlations and convolutions involved in the PP+PS=SS method. At the left, we can see how the cross correlation of the PP reflection  $X_A X_B$  with the PS event  $X_A X_D$  cancels out the downgoing P-wave leg of both events. The output is then convolved with a PS event propagating in the opposite direction that cancels out the remaining P-wave leg recorded at location  $X_B$ . Moreover, the traveltime of the upgoing S-wave leg recorded at  $X_C$  gets added to the one recorded at  $X_D$ . As a result, the SS traveltime between locations  $X_C$  and  $X_D$  is retrieved.

### Pseudo-shear-wave data in the rayparameter domain

Invoking the convolution theorem equation 14 can be written in the frequency domain as,

$$D_{\Psi S}(x_C|x_D, \omega) = \int \int D_{PS}(x_A|x_D, \omega) D_{PP}(x_A|x_B, \omega)^* D_{PS}(x_B|x_C, \omega) dx_A dx_B \quad (15)$$

$$= \int D_{PS}(x_A|x_D, \omega) D_{PP}(x_A|x_B, \omega)^* dx_A \int D_{PS}(x_B|x_C, \omega) dx_B, \quad (16)$$

The integration over  $dx_A$  can be easily identified as the cross correlation reciprocity equation (equation 3). From equation 7 we know that it can be solved in the  $\tau$ - $p$  domain. On the other hand, integration over  $dx_B$  with the output of the previous integral represent a convolution-type reciprocity equation. The latter can also be computed in the  $\tau$ - $p$  domain as shown in equation 12.

Figure 4 illustrates the processes involved in equation 16. The leftmost integral runs over positions  $x_A$  looking for the stationary position where the downgoing P-wave legs of the PP and PS events being cross correlated cancel. On the other hand, the second integral performs a convolution searching for the stationary position where the P-wave leg of the PS event originating at  $x_B$  cancels out the remaining P-wave traveltime from the previous integration while adding the S-wave traveltime from the interface to the surface. The final result is that all the P-wave legs get cancelled and the S-wave traveltimes get added.

### Numerical experiments

To test all the mathematical framework explained before, synthetic data were computed using a raytracing algorithm. Figure 5 shows the velocity model used for the ray tracing. The model is made of one flat interface at 1000 m depth, with constant P and S-wave velocities. Synthetic shot records were computed using 251 receivers with a 4m spacing, for a maximum offset of 1000 m. Figure 6 shows the vertical and horizontal component shot gathers with the PP and PS events recorded on each. Amplitudes have been normalized trace-by-trace to focus just on the kinematics of the events.

The first step to reconstruct pure S-wave traveltimes from PP and PS data in the plane-

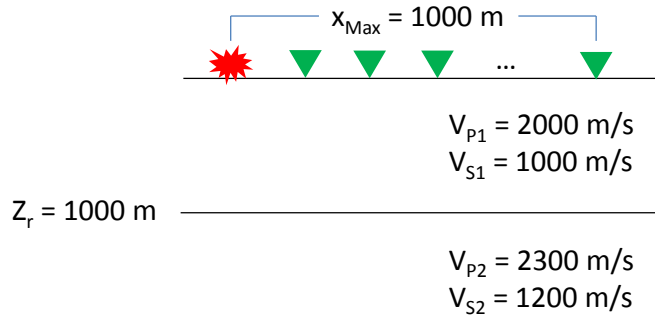


FIG. 5. Velocity model used for computing synthetic traces.

wave domain is to apply a  $\tau$ - $p$  transform to the input data. Figure 7 shows the input data transformed to the  $\tau$ - $p$  domain. The first thing we notice is that undesired events appear on the data. Two flat events at 1s and 1.5s on the PP and PS data are prominent. When working with convolution and cross correlation methods, care must be taking to assure that the data involved in these operations are actual events. Cross correlation of coherent numerical noise with the actual events may produce unphysical events in the output. Additional filtering may be needed in this case to remove the numerical artifacts introduced by the  $\tau$ - $p$  transform.

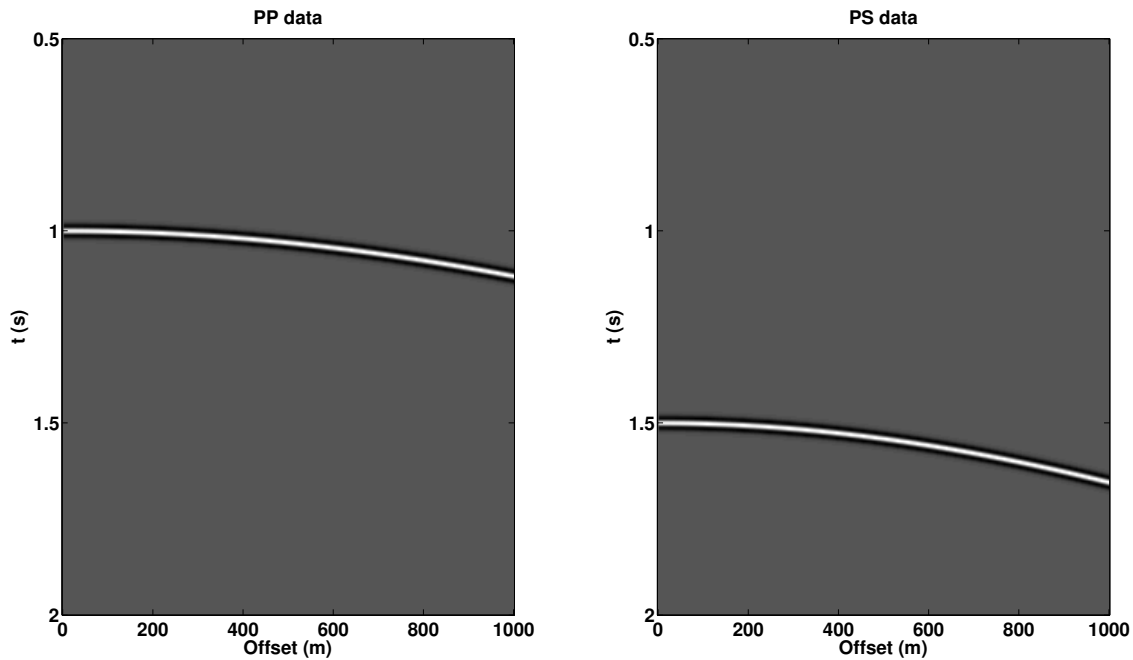


FIG. 6. PP (left) and PS (right) synthetic events computed by ray-tracing. Trace-by-trace normalization has been applied to focus just in the kinematics of the events.

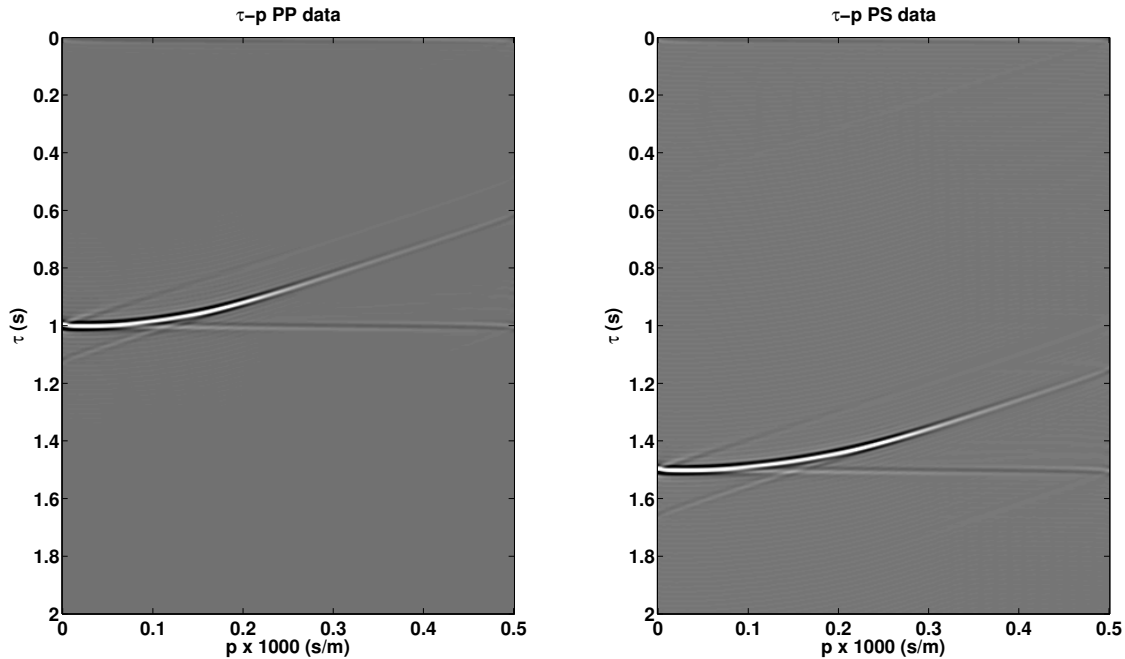


FIG. 7.  $\tau$ - $p$  transform of the synthetic data shown in Figure 6.

After cross correlating and convolving the  $\tau$ - $p$  data as discussed in the previous section we get what can be interpreted as the  $\tau$ - $p$  transform of the pseudo-shear-wave data we are trying to retrieve (Figure 8). It is important to note how the presence of the artifacts produced by the  $\tau$ - $p$  transformation has resulted in the generation of even more fake events, after cross correlations and convolutions have been computed.

Finally, the pseudo-shear-wave  $\tau$ - $p$  data are transformed back to the  $x$ - $t$  domain. The result of this is shown in Figure 9. There we can see how the retrieved SS data follows very closely the red line indicating the expected SS traveltimes. Both traveltimes begin to disagree for offsets larger than 550m. This is very close to the critical offset for PS conversions we expect from the velocity model used. Assuming a P-wave arriving with an incident angle of  $90^\circ$ , the maximum S-wave emergence angle can be computed following Snell's law as  $\theta_S^{crit} = \sin^{-1}(V_s/V_p)$ . The maximum offset we may expect for a SS reflection with that angle is  $x_{ss}^{crit} = Z \tan(\theta_S^{crit})$ , where  $Z$  is the depth to the interface. Plugging in the values we have in our model we get a maximum offset of 577m. Beyond that offset the retrieved traveltimes underestimate the actual SS traveltimes. This is a result of adding traveltimes that do not reach the angles required for an actual SS event at those offsets.

The scaling and filtering issues we can see in Figure 9 are beyond the scope of this work and will be addressed in a different study.

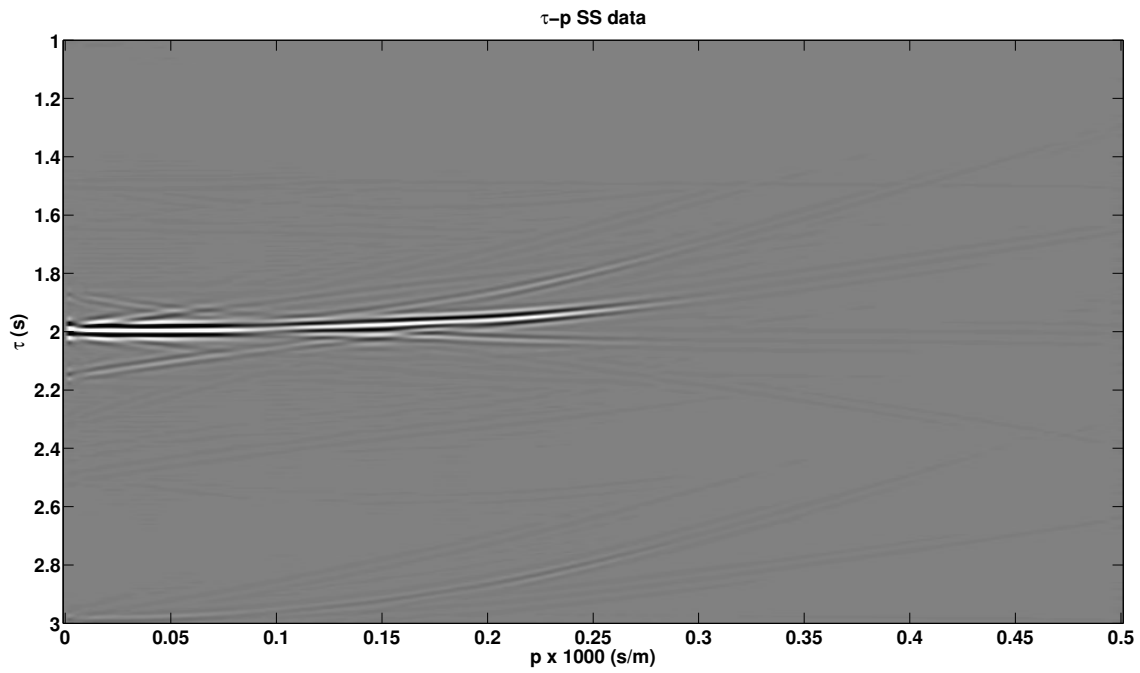


FIG. 8.  $\tau$ - $p$  transform of the pseudo-shear-wave data after performing all correlations and convolutions required for the PP+PS=SS method.

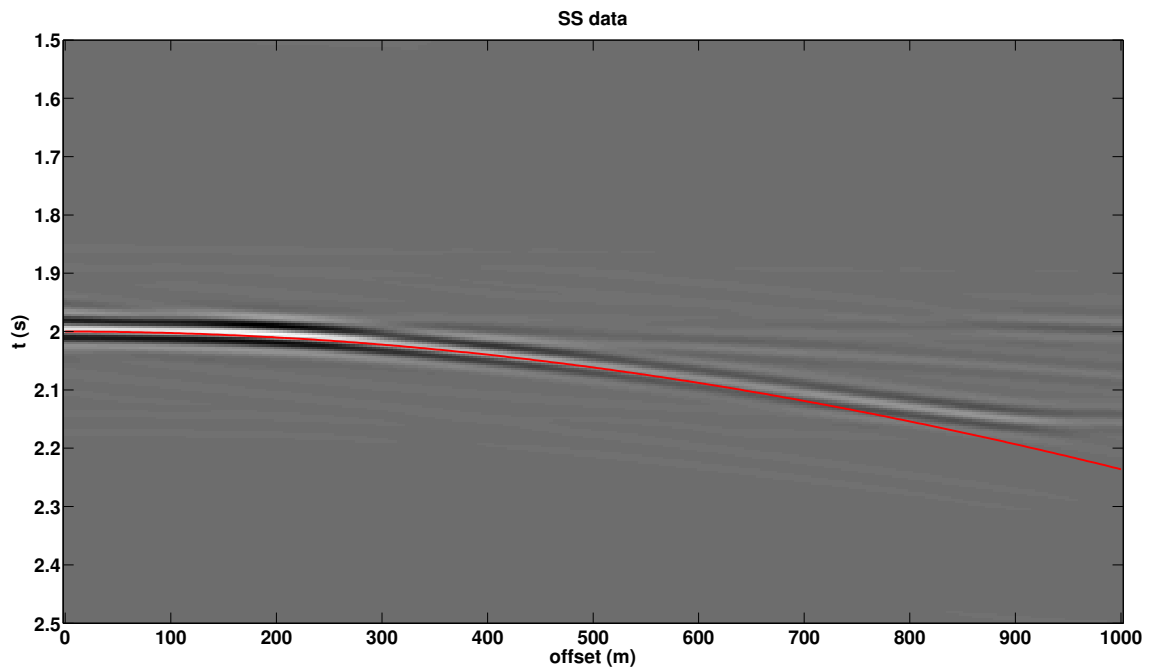


FIG. 9. Pseudo-shear-wave data after inverse transformation to the x-t domain. The red line indicates the expected SS traveltimes.

## CONCLUSIONS

The PP+PS=SS method in the plane-wave domain appears to be able to retrieve the kinematics of pure S-wave reflections given PP and PS data. This may be useful to simplify the processing and analysis of converted-wave data. Pure S-wave reflections can be processed using the same methods developed for P-waves, without the need for accounting for complicated asymmetrical raypaths.

For this method to be successful, the algorithm used for the  $\tau$ - $p$  transformation must be relatively free of artifacts. The PP+PS=SS method relies on the use of cross correlations and convolutions that predict new events from pre-existing ones. Hence, it is important that the input to this process only contain the events we need in the reconstruction. Otherwise, unphysical events or crosstalk will be present in the output data. Alternative ways of getting access to the rayparameter domain should be considered. Using a radial transform instead of a  $\tau$ - $p$  transform might alleviate the introduction of artifacts into the data, since it is an artifact-free, exactly invertible transform.

## ACKNOWLEDGEMENTS

The authors are grateful to Dave Henley for helping in the editing of this report. We also acknowledge CREWES sponsors and NSERC (Natural Science and Engineering Research Council of Canada) for providing the financial support for this research.

## REFERENCES

- Claerbout, J. F., 1975, Slant-stacks and radial traces: Stanford Expl. Project Report, **SEP-5**, 1–12.
- Grechka, V., and Dewangan, P., 2003, Generation and processing of pseudo-shear-wave data: Theory and case study: *Geophysics*, **68**, 1807–1816.
- Grechka, V., and Tsvankin, I., 2002, PP+PS=SS: *Geophysics*, **67**, 1961–1971.
- Schuster, G., 2009, *Seismic interferometry*: Cambridge University Press.
- Stoffa, P. L., 1989, *Tau-p: A plane wave approach to the analysis of seismic data*: Kluwer Academic Publishers.
- Tao, Y., and Sen, M. K., 2013, On a plane-wave based crosscorrelation-type seismic interferometry: *Geophysics*, **78**, No. 4, Q35–Q44.
- Wapenaar, K., 2004, Retrieving the elastodynamic Green's function of an arbitrary inhomogeneous medium by cross correlation: *Physical Review Letters*, **93**, 254,301.1–254,301.4.
- Wapenaar, K., van der Neut, J., Ruigrok, E., Draganov, D., Hunziker, J., Slob, E., Thorbecke, J., and Snieder, R., 2011, Seismic interferometry by crosscorrelation and by multidimensional deconvolution: a systematic comparison: *Geophysical Journal International*, **185**, No. 3, 1335–1364.